



# Aniline-based silane as a primer for corrosion inhibition of aluminium

D.O. Flamini<sup>a</sup>, M. Trueba<sup>b,\*</sup>, S.P. Trasatti<sup>b</sup>

<sup>a</sup> Department of Chemical Engineering, Universidad Nacional del Sur, Av. Alem 1253, 8000 Bahía Blanca, Argentina

<sup>b</sup> Department of Physical Chemistry and Electrochemistry, Università degli Studi di Milano, Via Golgi 19, 20133 Milan, Italy

## ARTICLE INFO

### Article history:

Received 19 May 2011

Received in revised form

30 September 2011

Accepted 7 November 2011

Available online 7 December 2011

### Keywords:

Aluminium

Corrosion protection

Silane-based treatments

Conducting polymers

## ABSTRACT

Hybrid films based on polyaniline and polysiloxane moieties were successfully deposited on commercial aluminium alloy using N-(3-trimethoxysilylpropyl)aniline (AnSi) as primer. The spectroscopic studies conducted on both the silane solution and the resulting films, jointly with several corrosion tests in NaCl, strongly support the protection performance of the hybrid films. The overall study demonstrates that typical silane-based treatments with principally barrier action can gain in active properties if the silane compound contains monomers of conducting polymers as a functional group.

© 2011 Elsevier B.V. All rights reserved.

## 1. Introduction

Aluminium and its alloys constitute the most important material, after steel, for various different practical applications. The presence of an adherent and thin oxide layer onto aluminium, imparts high corrosion resistance in moderately corrosive media. However, in aggressive environments, the thin oxide film does not provide long-term corrosion resistance, resulting in localized attack of the substrate surface [1]. Therefore, different coating treatments of the aluminium surface are required to obtain major protection levels.

Varied conversion coatings were used for corrosion prevention. For example, chromating and chromium passivation provide good corrosion resistance for aluminium and its alloys [2,3]. However, the toxicity associated with hexavalent chromium generated by the residues of the chromating process requires new chromium-free technologies. The corrosion inhibition of aluminium alloys has conditioned the development of several alternatives, among which conducting polymers (CPs) are intensively investigated as active coatings [4–10]. The protection capabilities of CPs are strongly influenced by the nature and surface preparation of the metal substrate, as well as by the CP characteristics and method of deposition. The low processability and poor adhesion to active metals, as well as the inherent porosity at molecular level with fast cation incorporation during the corrosion-induced CP reduction, limit their use as contiguous polymer films [11–13]. Our recent

work dealing with polypyrrole electro-deposited on different Al alloys, namely, AA6082, AA5083-H111 and AA2024-T3, highlights also the role of the rate at which structural and conformational changes are driven within the polymer network [13]. Overall the suggested mechanism(s) for corrosion protection by CPs (anodic protection/passivation, ennobling, galvanic/barrier protection, galvanic/redox inhibition), still highly debated for aluminium alloys, galvanic coupling between metal and CP and the latter re-oxidation assisted by oxygen appear to play a key role in ensuring an effective corrosion inhibition [14–17].

One of the recent treatments employed to replace chromium-based coatings consists in silane technology, where electrochemical participation of the metal in the silane-based film deposition mechanism is not necessary [18–21]. Silanes are hybrid molecules containing functional organic groups attached to inorganic silicon atoms. By dipping the metal in a silane hydrolyzed solution, silanol groups Si–OH react with hydroxide groups on the substrate surface to form hydrogen bonds [22]. During subsequent thermal treatment, water elimination and covalent bonding at the film/metal interface (Si–O–Me) occur. Also, crosslinking and branching are favored thus obtaining a dense siloxane Si–O–Si network, that limits the access of aggressive species to the underlying metal. Nevertheless, for an effective barrier against corrosion, high hydrophobicity is necessary to limit water permeation. In contrast to conducting polymers, the most explored silanes do not provide active action and doping with substances having inhibiting properties is needed [21,23].

A few years ago, we have developed a new approach that allows to obtain an hybrid film containing polypyrrole units and polysiloxane linkages in a simple way, using a pyrrole-based silane as a

\* Corresponding author. Tel.: +39 0250314207; fax: +39 0250314300.  
E-mail address: [monica.trueba@unimi.it](mailto:monica.trueba@unimi.it) (M. Trueba).

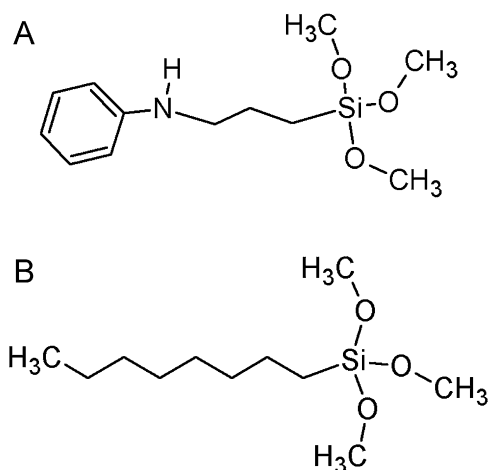


**Fig. 1.** (a) N-(3-trimethoxysilylpropyl)aniline (AniSi); (b) n-octyltrimethoxysilane (OcSi).

primer on as-received wrought Al alloys [24]. The outstanding performance was attributed to a synergistic effect in terms of adhesion, compactness and passive/active actions against metal degradation as a result of polypyrrole and polysiloxane interlinking in a single macromolecular network. Last but not least, hybrid coating deposition was carried out following the conventional steps for silanes deposition [23] consisting of dipping the metal in the hydrolysed primer solution and curing (thermal treatment). To acquire deeper knowledge on the protection capabilities of silane molecules functionalized with a monomer of a conducting polymer, aniline-based silane (AniSi) was investigated (Fig. 1a). Also, the distinct doping mechanism of aniline in relation to the limited oxidation/protonation of N-substituted aniline [25–27], could help to understand better the role of the conducting polymer moieties within the macromolecular hybrid network.

This work reports on the surface treatment of a commercial-purity aluminium alloy AA1050 with AniSi hydrolyzed solution, according to the above-mentioned procedure. AniSi solution and as-deposited PAniSi films were characterized by UV–visible and reflection-absorption IR spectroscopy, respectively. Corrosion protection was evaluated in a near neutral 0.6M NaCl solution by several electrochemical experiments. In parallel, n-octyltrimethoxysilane (OcSi) of molecular weight comparable to that of AniSi, but with different organic functionality, was also investigated as a reference system (Fig. 1b).

## 2. Experimental

### 2.1. Materials

The material used in this work was commercial-purity aluminium with 99.5% Al, denominated as AA 1050 H24, according to the ASTM-Standard [28]. The nominal composition is reported in Table 1. The material was purchased from AVIOMETAL S.p.A. in the form of sheets of 1.5 mm thickness, which were cut into 20 mm × 50 mm coupons. Prior to testing, the surface was degreased by sonication in three different solvents: n-hexane, acetone and methanol, respectively, 15 min each.

**Table 1**  
Chemical composition (wt%) of commercial aluminium AA1050-H24.

Si	Fe	Cu	Mn	Mg	Zn	Ti	Cr	Al
0.14	0.25	< 0.01	0.01	< 0.01	< 0.01	0.01	< 0.01	Balance

**Table 2**

Experimental conditions for surface treatment with silane-based hydrolysed solutions.

Film designation	Silane solution <sup>a</sup>	Immersion time (min)	Curing time (min)
PAniSi	AnSi <sup>b</sup>	3	60
PAniSi-R	AnSi-R <sup>c</sup>	3	60
PAniSi <sup>M</sup>	AnSi	1 (×3) <sup>d</sup>	20 (×3) <sup>d</sup>
PAniSi-R <sup>M</sup>	AnSi-R	1 (×3)	20 (×3)
POcSi	OcSi <sup>b</sup>	3	60
POcSi <sup>M</sup>	OcSi	1 (×3)	20 (×3)

<sup>a</sup> Metal substrates were cleaned in ultrasound bath with hexane, acetone and methanol (15 min each), pre-heated for 20 min (130 °C) in open to air sand oven, and then immersed in the silane solution (4 vol% in MetOH/H<sub>2</sub>O 95:5; pH 4.6).

<sup>b</sup> Used after 3 days of its preparation.

<sup>c</sup> Used after 10 days of its preparation (pink-colored solution).

<sup>d</sup> Multiple layer deposition: three immersions for 1 min., each followed by curing for 20 min.

All chemicals were of analytical reagent grade and used as received. Millipore MilliQ<sup>®</sup> water was used to prepare solutions.

### 2.2. Coatings deposition

AniSi and OcSi hydrolysed solutions were prepared at 4 vol.% in methanol/water (95:5), with pH adjusted to 4.6 by adding acetic acid, and left under stagnant conditions for three days before use. Freshly prepared AniSi solution was also used after 10 days (AniSi-R), the time at which pink coloration was clearly developed. Cleaned and pre-heated Al specimens were modified with the silanes by single and multiple immersions in the hydrolysed solutions, followed by curing in an open-to-air sand oven, as reported in Table 2. Coated specimens, designated as PAniSi, PAniSi-R and POcSi, were stored in a desiccator before the experiments.

### 2.3. Characterization of silane-based solution and coatings

Silane-based hydrolyzed solutions were characterized by recording UV–vis spectra as a function of time, using a JASCO V530 spectrometer in the wavelength scan mode in the region 200–800 nm. 10 mL of silane stock-solutions, prepared as reported above, were used to fill the standard 10 mm path length quartz cell each time. Reflection–Absorption IR (RAIR) spectroscopy was used for coating structural characterization using a Spectrum One (PerkinElmer) spectrophotometer in 4000–400 cm<sup>-1</sup> range (64 scans) with a spectral resolution of 4 cm<sup>-1</sup>. RAIR spectra were recorded at different incidence angles (30°, 45° and 75°). The surface composition of PAniSi coatings was analysed by X-ray photoelectron spectroscopy (XPS) using a ESCA system (XI ASC II Surface Science Instruments) at operating pressure between 10<sup>-8</sup> and 10<sup>-9</sup> Torr, fitted with Al anode (1486.6 eV) and 1 eV energy resolution. The morphology of the coatings was examined on a scanning electron microscopy (SEM), using a 1430 LEO microscope with a chamber pressure of 8 × 10<sup>-6</sup> Torr and 20 keV accelerating voltage.

### 2.4. Corrosion tests

Experiments were performed in naturally aerated 0.6 M NaCl solutions (pH 6.5 ± 0.2) prepared with reagent grade NaCl (98%, Aldrich). The corrosion performance of bare and coated specimens

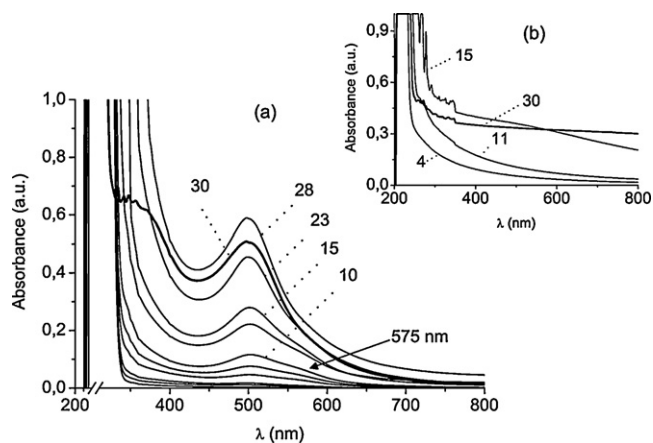


**Fig. 2.** UV-vis absorption spectra as a function of time of (a) AniSi and (b) OcSi solutions, prepared at 4 vol% in MetOH/H<sub>2</sub>O 95:5; pH 4.6. Numbers indicate the time (in days). Absorptions were normalized to 1.

was studied at room temperature by several conventional corrosion experiments. Cyclic anodic potentiodynamic polarization curves with a scan rate of 10 mV min<sup>-1</sup> were recorded from the open circuit potential ( $E_{ocp}$ ), after an equilibration of 10 min in the test solution, up to  $5 \times 10^{-3}$  A cm<sup>-2</sup>. The direction of the scan was then reversed into the active direction up to complete repassivation, indicated by the potential at which the current density reaches its lowest anodic value. Cathodic polarizations up to  $-5 \times 10^{-3}$  A cm<sup>-2</sup> were similarly recorded using freshly prepared samples. The open circuit potential of bare and coated samples was monitored as a function of time during 15 h. The same time interval was used for recording current responses at the pitting potential of the bare alloy ( $E_{pit} = -700$  mV vs. SCE) that was previously determined as described elsewhere [29].

All measurements were performed using a single-compartment O-ring cell [24,29] with a working (active) surface area of 1 cm<sup>2</sup>. A Pt sheet was used as a counter electrode, and a saturated calomel electrode (SCE) connected to the working compartment via a salt bridge containing the test solution and a Luggin capillary, as a reference electrode. Data were recorded by means of a PAR Model 273A potentiostat-galvanostat using a SoftCorr<sup>TM</sup> II software.

Long-term immersion tests were performed on bare, POcSi and PAniSi coated samples at room temperature for a period of 30 days, according to ASTM G31 recommendations [30].

### 3. Results and discussion

#### 3.1. Silane solutions and film characterization

UV-vis absorption spectra of AniSi and octylsilane (OcSi) as a function of time (up to 1 month) are shown in Fig. 2a and b. It can be appreciated that AniSi solution spectra differs importantly from those of OcSi. The main spectral features of OcSi are revealed at wavelengths ( $\lambda$ ) below 400 nm, while AniSi exhibits a distinct broad absorption peak at 500 nm. In the case of OcSi (Fig. 2b), the bathochromic shift and narrowing of the absorption bands with time indicate the reduction of HOMO-LUMO gap as a result of  $\sigma$ - $n$  mixing (silicon  $\sigma$ -oxygen  $n$  orbital interactions) and the formation of octylsiloxane chains with regular backbone structure [31]. The splitting of the transitions reflects the formation of siloxane segments of variable lengths and/or conformations, while larger insoluble oligomers are indicated by the decrease of absorption after one month. Also, a red shift of the absorption tail up to  $\lambda$  of about 450 nm is obtained with AniSi solution (Fig. 2a), but it is featured by a distinct intensity increase. This reflects the

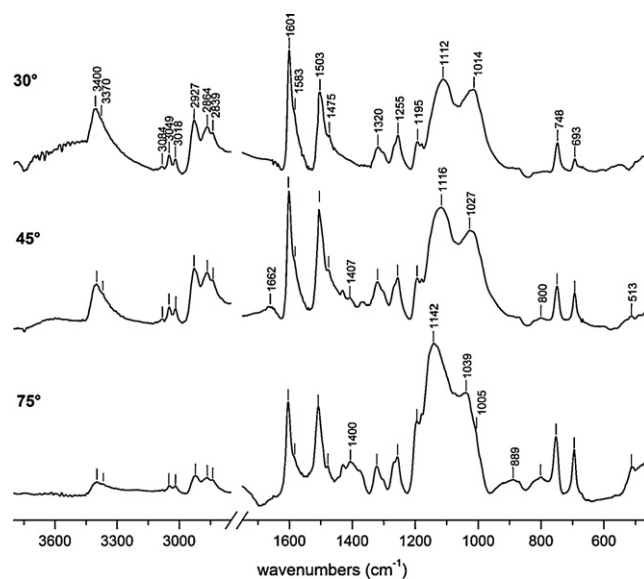


**Fig. 3.** RAIIR spectra at increasing incidence angles (from top to bottom) of PAniSi/AA1050.

decrease of the HOMO-LUMO energy gap due to higher electron delocalization that results from  $\sigma$ - $\pi$  mixing effect and  $\pi$ - $\pi^*$  interactions, rather than  $\sigma$ - $n$  mixing effect [32–34]. In addition, the broad band with a well-defined maximum at 500 nm that progressively grows and expands towards the near IR region, in part due to the weak shoulder at about 575 nm, suggests the formation of chemical species that stabilize the reactive system. In concomitance, AniSi solution started to acquire pink coloration that was clearly visible after 10 days. These observations indicate that intermolecular polarization and/or polarization effects induced by the local environment [32] promote the formation in AniSi solution of radical cations of type  $C_6H_5NH^{+\bullet}(CH_2)_3Si(OH)_3$  possibly stabilized by the negative charge located on the silanol group [35,36]. The formation of small benzenoid/quinoid aniline “head-to-tail” oligomers, indicated by the emerging shoulder at 575 nm, however, is limited and association processes through hydrogen bonds prevail (peak at 500 nm) [27,35]. Accordingly, charge-transfer H-complexes assisted by proton exchange between radical cations and neutral radicals ( $NH^{+\bullet} \leftrightarrow N^{\bullet} + H^+$ ) of aniline rings in the hybrids, become the prevailing species in AniSi solution with time. This could also justify the almost constant pH with time of AniSi solution. Near IR absorption could result as well from amino group interaction via  $SiO^-$  through hydrogen bonds [37], but such interaction is less favored due to electronic and steric constraints. In fact, as for OcSi solution (Fig. 2b), absorbance importantly decreases after 30 days, in particular at wavelengths below 400 nm, indicating insoluble hybrid AniSi oligomers in solution due to the formation of larger siloxane segments.

As deposited POcSi and PAniSi films on AA1050 surface were quite uniform and bright at naked eyes, but for the latter slight-brownish appearance was also noticed upon visual inspection. Previous studies of POcSi films by RAIIR spectroscopy have revealed disordered and incomplete cross-linked polysiloxane structures, even though cross-section SEM examination showed film thicknesses of about 5  $\mu$ m when 3 min single immersion in OcSi solution is carried out [38]. It was not possible to estimate the thickness of PAniSi film specimens because a distinguishable metal/film interface was not observed. It could be argued that the presence of aniline H-aggregates, providing higher hydrophobicity to AniSi solution, in contrast to OcSi, accounts for the former stronger interactions with the metallic surface. RAIIR spectra obtained at three

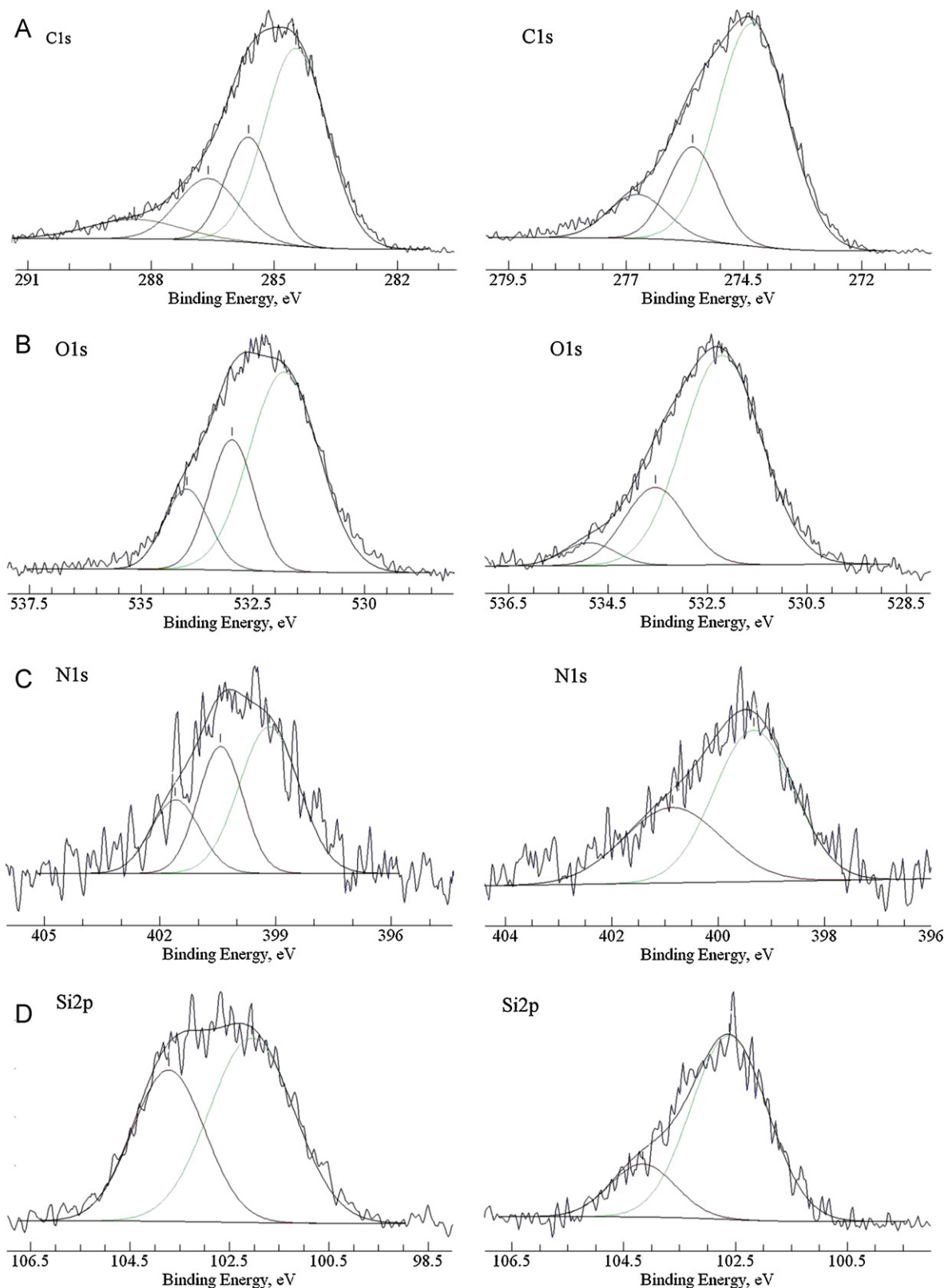


Fig. 4. XPS high resolution analysis of PANiSi (left) and PANiSi-R (right) films on AA1050: (a) C1s; (b) O1s; (c) N1s; (d) Si2p.

different incidence angles of PANiSi/AA1050 are shown in Fig. 3. In general, the spectra are quite similar and suggest homogeneous PANiSi structure with siloxane and aniline linkages throughout the film thickness [39–42]. The presence of siloxane chains is straightforwardly indicated by siloxane asymmetric stretching vibrations,

$\nu_a(\text{Si-O-Si})$ , in the  $1150\text{--}1000\text{ cm}^{-1}$  region with two maxima at about  $1120$  and  $1030\text{ cm}^{-1}$ . At higher incidence angle ( $75^\circ$ ), the former maximum prevails and is shifted to higher frequencies, which suggests prevalent linear arrangement of siloxane chains near the metal surface. Covalent bonding with the latter is suggested by

**Table 3**  
High-resolution XPS analysis of PAniSi and PaniSi-R films on Al alloy AA1050.

Photopeak	PAniSi/AA1050			PAniSi-R/AA1050			Chemical assignment
	BE <sup>a</sup> (eV)	FWMH <sup>a</sup> (eV)	Intensity (%)	BE (eV)	FWMH (eV)	Intensity (%)	
C1s	284.5	1.8	55	284.3	1.8	68	C–C, C–H, C–H <sub>2</sub>
	285.6	1.3	21	285.6	1.3	20	C–NH <sup>+</sup> , C–N <sup>+</sup> –
	286.6	1.8	16	286.8	1.5	11	C=N <sup>+</sup> –
	288.4	2.6	8	–	–	–	O=C–O
O1s	531.8	1.8	60	532.2	1.9	73	O–Si–C
	533.0	1.2	25	533.6	1.5	21	SiO <sub>2</sub>
	534.0	1.2	15	534.9	1.2	5	O=C–O
N1s	399.2	1.8	49	399.3	1.8	62	–NH
	400.4	1.4	31	400.9	2.1	38	–NH <sup>+</sup> , –N <sup>+</sup> –
	401.6	1.5	20	–	–	–	=N <sup>+</sup> –
Si2p	102.1	2.0	59	102.6	1.6	80	C–Si–O
	103.7	1.7	41	104.2	1.4	20	SiO <sub>2</sub>

<sup>a</sup> BE – binding energy; FWMH – full width at half-maximum height.

Si–O–Al vibrations at about 1000 cm<sup>-1</sup>. N-substituted aniline moieties dominate the spectral features in the high (3000–3550 cm<sup>-1</sup>) and low (1660–1150 cm<sup>-1</sup> and 950–600 cm<sup>-1</sup>) frequency regions. The peak at about 3400 cm<sup>-1</sup>, associated with NH stretching, is tailed towards lower frequencies with a shoulder at ~3370 cm<sup>-1</sup>, strongly suggesting the formation of H-complexes [42]. In the low frequency region, the two peaks at 750 and 695 cm<sup>-1</sup> reveal terminal phenyl rings. Nevertheless, the weak band at ~800 cm<sup>-1</sup> is characteristic of para-disubstitution (“head-to-tail” coupling), while quinoid structures are clearly indicated by the inner weak shoulder near the strong peak at 1600 cm<sup>-1</sup> and the weak band at ~1660 cm<sup>-1</sup>. Carbonyl vibration (~1720 cm<sup>-1</sup>) associated to acetate ions (presumable dopants) is very weak, indicating low level of oxidation. This in part could be due to self-doping as a result of H-aggregation of aniline rings, in correlation with above-mentioned N–H stretching features. This result also agrees with UV–vis characteristics of AniSi solution discussed herein. Propyl chains tethering the oligosiloxane and oligoaniline moieties is confirmed by the characteristic –CH<sub>2</sub> stretching vibrations between 2950 and 2750 cm<sup>-1</sup>. Although no conformational order of propyl chains is revealed due to the absence of a sharp peak at ~720 cm<sup>-1</sup> [24], the decrease in intensity of the former bands in relation to ν<sub>a</sub>(Si–O–Si) between 1200 and 1000 cm<sup>-1</sup> as the incidence angle changes from 45° to 75° (Fig. 3), indicates that aromatic moieties are mainly tethered towards the film surface. However, aromatic ring–Al interaction is also suggested from the spectrum recorded at 75° by the broad band with several overlapping components between 1450 and 1350 cm<sup>-1</sup> and the weak feature at ~930 cm<sup>-1</sup> [42]. PAniSi-R film, obtained by AA1050 treatment with 10 days aged AniSi solution, showed similar spectral features to those discussed here-above, in contrast to XPS results.

XPS survey spectra of PAniSi and PAniSi-R films showed C1s, O1s, N1s and Si2p as the main peaks. However, higher surface concentrations (at%) of C and N were obtained in the latter film. The results of high resolution analysis are given in Fig. 4 and Table 3 [43–46]. It is important to note that no imine-like structure (=N– at ~398 eV) but neutral amine and charge-deficient N species (binding energy BE > 400 eV) prevail in both films, in agreement with the expected oxidized salt-like forms in N-substituted polyanilines [43]. However, as deduced for PAniSi from RAIR spectra (Fig. 3), low level of doping is further indicated by the low intensity of the signals associated to acetate species (~289 eV in C1s and 534 eV in O1s lines) in relation to positively charged nitrogen species. Accordingly, the non-uniform charge distribution on N atoms is attributed to H-bonding effects producing charge-transfer complexes that involve radical cations (–N<sup>•+</sup>) and NH groups with self-doping action [35]. When the alloy is modified with the

pink-colored AniSi solution (PAniSi-R film), the features of the high energy peaks in all element lines change appreciable (Fig. 4, right). In particular, the contribution of siloxane and acetate in the O1s line, and that of the former in the Si2p line are much less intense and occur at higher binding energies (Table 3). In addition, acetate species are not resolved for the C1s line and charge-deficient nitrogen species in the N1s line are more delocalized. All these features support the proposed H-aggregation of aniline units with time according to UV–vis results (Fig. 2a) and indicate that PAniSi-R films are thicker but less homogeneous in terms of network three-dimensional crosslinking via siloxane and aniline units with the latter mainly oriented towards the film surface.

### 3.2. Protection performance

Single-cycle anodic polarization scans for bare and POCsi-coated AA1050 are shown in Fig. 5. Some protection is indicated by the positive shift of the forward curves in more than 100 mV with respect to that of the bare substrate, featured by several regions of current stabilization with potential. However, the latter is absent at the beginning of the scan, which reflects limited barrier-type action. In addition, the cyclic curve of POCsi<sup>M</sup>-coated alloy (multiple layer approach, see Table 2) almost replicates that obtained by single immersion/curing procedure, indicating limited substratum defects concealing through layer-by-layer deposition. In the case of PAniSi-coated specimens (Fig. 6), forward scans are notably

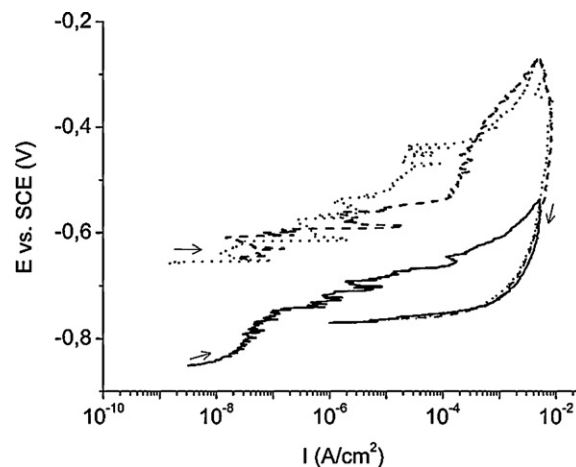


**Fig. 5.** Single-cycle anodic polarization scans (10 mV min<sup>-1</sup>) in naturally aerated 0.6 M NaCl (pH 6.5 ± 0.2) from *E*<sub>ocp</sub> after 10 min of equilibration in the test solution: (–) bare AA1050; (– –) POCsi/AA1050; (· · ·) POCsi<sup>M</sup>/AA1050.

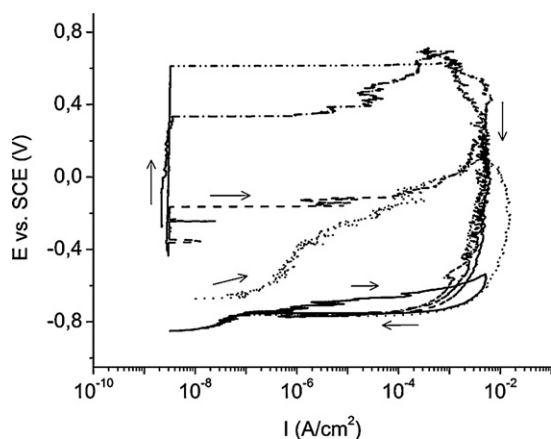


**Fig. 6.** Single-cycle anodic polarization scans ( $10 \text{ mV min}^{-1}$ ) in naturally aerated  $0.6 \text{ M NaCl}$  ( $\text{pH } 6.5 \pm 0.2$ ): (—) bare AA1050; (---) PAniSi/AA1050; (- - -) PAniSi<sup>M</sup>/AA1050; (· · · ·) PAniSi-R/AA1050; (- · · · ·) PAniSi-R<sup>M</sup>/AA1050.

shifted to higher potentials, in particular as multiple layer deposition is used (Table 2). Thus, the concealing effect is much more significant with respect to OcSi treatment. Passive regions at about  $10^{-9} \text{ A cm}^{-2}$  in a wide range of less negative potentials with the breakdown shifted near  $1 \text{ V}$  from that of the bare alloy are obtained for almost all coated substrates except when the alloy is treated once with Anisi-R solution. The latter shows a loop-like passivity due to a more porous and/or less homogeneous hybrid network. This, however, can explain the better interconnection between multiple layers as reflected by the highest ennobling obtained with PAniSi-R<sup>M</sup>/AA1050. Semipassivation regions or metastable-like macro-pitting, attributed to re-oxidation of aniline moieties within the coatings due to their active action in Al oxide regeneration [24], are only revealed as the alloy is modified with fresh Anisi solution, which correlates with the lower contribution of charge deficient N species on the PAniSi film (Table 3). The reverse scan is shifted to lower currents at potentials below the bare alloy breakdown, suggesting less difficult repassivation of corroded surfaces.

Separate samples of bare AA1050 and the substrate treated with POcSi, PAniSi and PAniSi-R were subjected to cathodic polarization to further evaluate the performance of the coatings obtained by single immersion/curing in the corresponding silane solution. In Fig. 7, it can be appreciated that the cathodic curve of POcSi-coated alloy is shifted to lower current values, thus reflecting

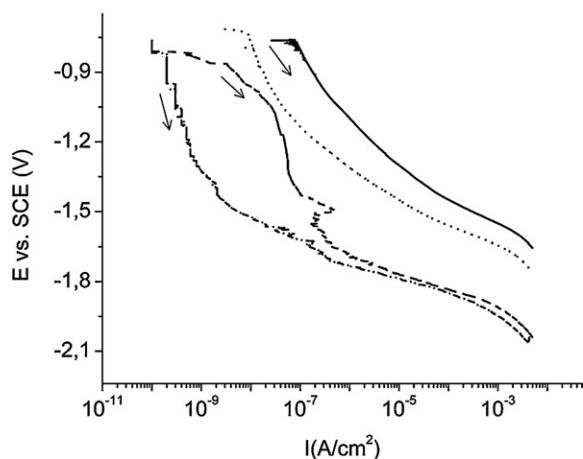


**Fig. 7.** Cathodic polarization scans ( $10 \text{ mV min}^{-1}$ ) in naturally aerated  $0.6 \text{ M NaCl}$  ( $\text{pH } 6.5 \pm 0.2$ ) from  $E_{\text{ocp}}$  after 10 min of equilibration in the test solution: (—) bare AA1050; (· · · ·) POcSi/AA1050; (- · · · ·) PAniSi/AA1050; (- - -) PAniSi-R/AA1050.

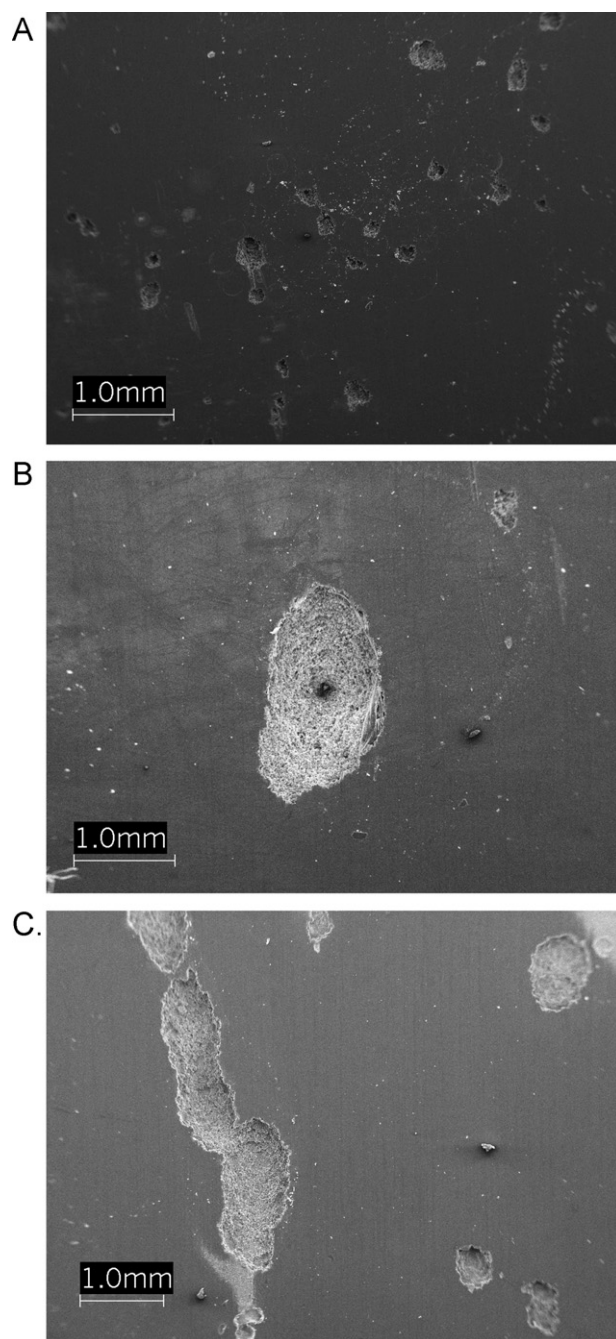


**Fig. 8.** Surface SEM images of bare and Anisi-modified AA1050 after cathodic polarizations (Fig. 7): (a) bare AA1050; (b) PAniSi/AA1050; (c) PAniSi-R/AA1050.

delayed cathodic processes of oxygen reduction and hydrogen evolution. However, these reactions are substantially retarded with PAniSi-based films, notwithstanding the higher porosity of PAniSi-R, pointing out the superior performance of the hybrid coatings over more hydrophobic conventional organofunctional silane. The cathodic curve of PAniSi-R/AA1050 shows a distinct current peak at about  $-1.5 \text{ V}$ , which suggests a transition from conductive state to a less conductive form of aniline moieties within the hybrid network. Such feature was observed for polyaniline films on AA2024 and was attributed to transition from emeraldine salt to non-conductive leucoemeraldine by coupling with the metal substrate [14]. The conductive state transition is likely suggested also on PAniSi/AA1050, though more smoothly due to more compact coating structure, being thus masked by the cathodic reactions. SEM

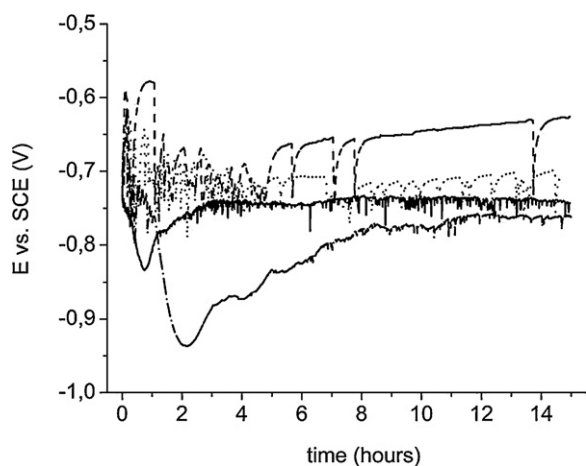


**Fig. 9.** Open circuit potential monitoring up to 15 hours in naturally aerated 0.6 M NaCl (pH  $6.5 \pm 0.2$ ): (—) bare AA1050; (---) POCs/AA1050; (···) PAniSi/AA1050; (-·-·) PAniSi-R/AA1050.

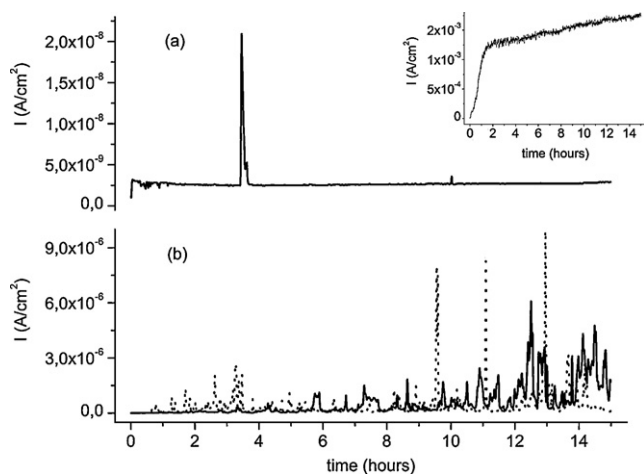


**Fig. 10.** Current responses at the pitting potential of the bare AA1050 ( $E_{\text{pit}} = -700 \text{ mV vs. SCE}$ ) during 15 hours in naturally aerated 0.6 M NaCl (pH  $6.5 \pm 0.2$ ): (a) PAniSi/AA1050, inset – bare alloy; (b) (—) PAniSi-R/AA1050, (···) POCs/AA1050.

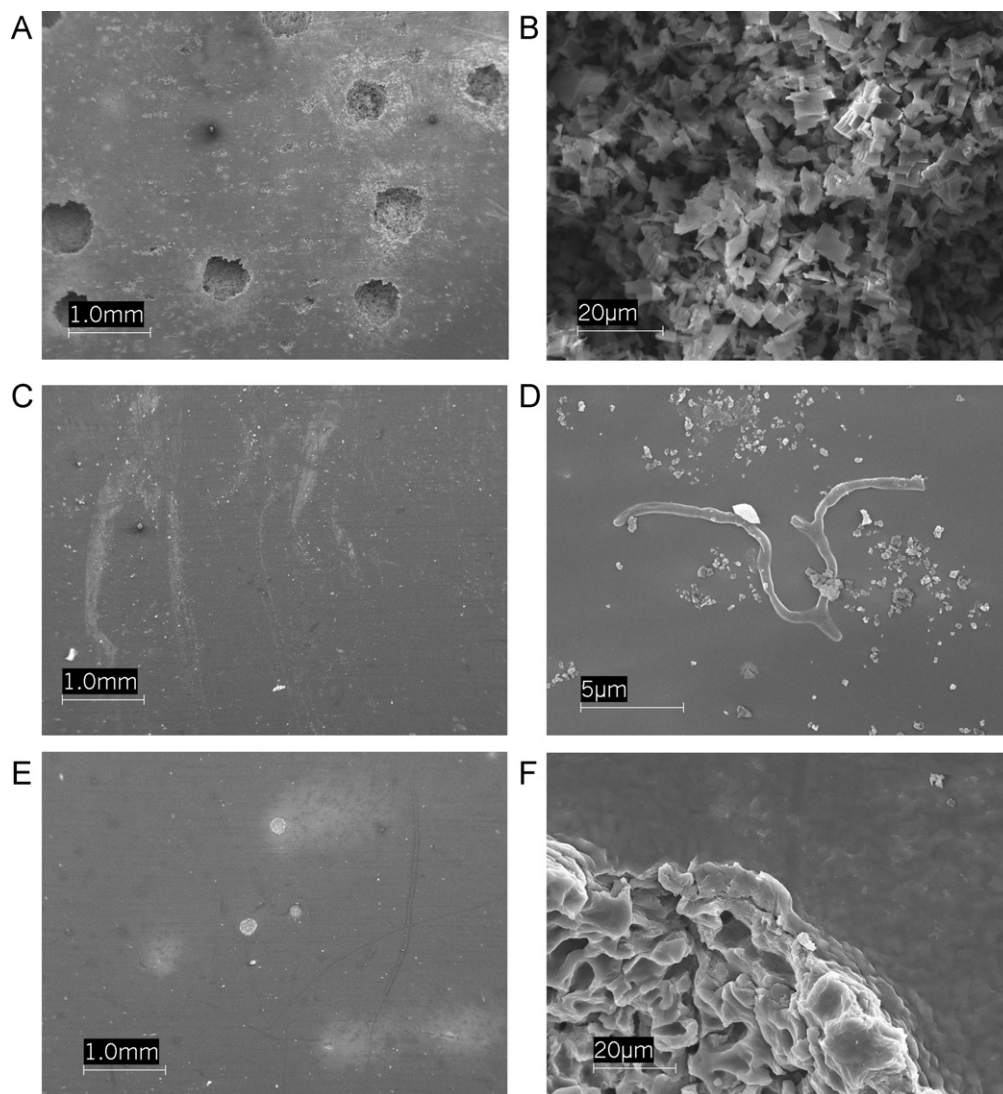


**Fig. 11.** Surface SEM images of bare and Anisi-modified AA1050 after potentiostatic experiment (Fig. 10): (a and b) bare AA1050; (c and d) PAniSi/AA1050; (e and f) PAniSi-R/AA1050.

morphology examination of bare and PAniSi-coated specimens showed more locally damaged sites, while pitting attack prevailed on the uncoated alloy, as shown in Fig. 8. A very deep crater-like corroded site featured PAniSi/AA1050 specimen, reflecting highly adhered compact hybrid film virtually free from gross defects. Instead, the higher permeability of PAniSi-R film was clearly manifested by larger attacked zones.

Since anodic and cathodic polarizations can over-estimate the protection capabilities of these coatings by promoting the oxidation and reduction, respectively, of oligoanilines within the hybrid network, additional tests were carried out and discussed here below.

Fig. 9 shows the time-dependent response of the open circuit potential ( $E_{ocp}$ ) for bare and coated AA1050 substrates. The overall response of POCsi/AA1050 is similar to that of the bare alloy but the initial decay of  $E_{ocp}$  to more negative potentials lasts longer, passing through the minimum at about 2 h. After this time, the potential tends to level off close to that of bare AA1050 ( $\approx -750$  mV). This indicates that POCsi film does not prevent corrosion of the substrate for long time in the given aggressive media. Immersion in NaCl solution during 30 days confirmed this result, which was indicated by the appreciable deterioration of the film observed at the end of the test. Both PAniSi-coated specimens also show an initial decay of  $E_{ocp}$  but up to values close to that of bare alloy. Thereafter, the potential progressively shifts to more positive values, especially for PAniSi/AA1050. Although strong negative potential transients characterize the  $E_{ocp}$  variation, these are much more frequent in PAniSi-R-coated alloy, in correlation with the higher permeability of this film. The transients of  $E_{ocp}$  to the rest potential of bare alloy reflect gradual improvement of barrier protection as a result of metal coupling with aniline units [14,16]. The results further point out the remarkable protection of AA1050 by hybrid films, mainly due to improved barrier action by the three-dimensional hybrid network containing aniline oligomers, which provide a repairing effect. Long-term immersion tests (30 days in NaCl solution) confirmed the very good performance of PAniSi films in comparison to POCsi/AA1050, as manifested by some opacity due to corrosion products on the latter surface and the prevailing metallic-like appearance of PAniSi-coated substrates at the end of the experiment.

Potentiostatic experiments that consisted in recording for 15 h the current responses of bare and coated substrates polarized at the pitting potential of the bare alloy ( $E_{pit} = -700$  mV vs. SCE), were also carried out. The results are summarized in Fig. 10 and give decisive evidence in outstanding the corrosion inhibition of hybrid coatings. The current recorded on PAniSi/AA1050 (Fig. 10a) is almost constant at very low values (in the order of nanoampere) at all times; only few transients to higher current are observed. Conversely, the  $I-t$  response of PAniSi-R coated alloy is featured by many transients that progressively intensify, especially after about 8 h (Fig. 10b). However, notwithstanding the higher permeability of this film, the performance is better than that obtained with POCsi, whose  $I-t$  response is featured by very sharp current spikes up to  $\sim 10^{-5}$  A cm $^{-2}$  at shorter times (dotted line in Fig. 10b). Thus, taking into account the  $I-t$  response of the bare alloy (Fig. 10a, inset), POCsi film provides some protection but this fails at longer times, in agreement with the trend of  $E_{ocp}$  with time and long-term immersion tests.

The here-above observations were supported by surface morphology analysis of the specimens at the end of tests. No appreciable damage and few localized attacked sites were observed on PAniSi and PAniSi-R coated substrates, respectively, as compared to bare alloy (Fig. 11). At higher magnifications it was revealed that the attack on PAniSi/AA1050 is quite superficial with prevailing filliform-like corroded paths (Fig. 11d). The small corrosion products on the film surface reflect negligible coating defects, consistently with the excellent film compactness. More permeable

PAniSi-R film shows more spread undercoating attack (Fig. 11f), but the morphology of corroded sites differs from the characteristic metallographic pitting of bare AA1050 (Fig. 11b). This could suggest a different mechanism of alloy degradation, more probably due to active interaction of aniline moieties in the hybrid coating with the metallic substrate.

### 3.3. Conclusions

A simple procedure allowed to obtain hybrid PAniSi films on Al alloy AA1050 using an aniline-based silane as a primer. Anisi solution characterization indicated that macro-agglomerates composed by siloxane and aniline oligomers, the latter mainly stabilized as H-complexes, are formed in solution. Upon surface modification, crosslinking of self-assembled macromolecules is further promoted, thus obtaining the PAniSi hybrid network. The optimal performance against AA1050 corrosion with respect to POCsi film is due not only to the improved adhesion by silanol adsorption/condensation at the metal surface and the high compactness due to three-dimensional cross-linking. Aniline moieties/oligomers in the hybrid film act likely on demand against AA1050 degradation as barrier protection fails and/or permeability increases. The latter is clearly manifested when the alloy is treated with aged Anisi solution with higher contribution of hydrophilic paths. These results support our previous studies dealing with protective properties of polysiloxane-based coatings through silane molecule functionalization with a pyrrole ring. From a conceptual point of view, the synergistic effect of combining monomers of conducting polymers and silane functionalities at a molecular level is demonstrated. This approach would constitute a valid alternative to hexavalent chromium treatments in practical applications.

### Acknowledgments

The financial support of the Secretaría de Ciencia y Técnica (Universidad Nacional del Sur), the Consejo Nacional de Investigaciones Científicas y Técnicas (CONICET) are gratefully acknowledged.

### References

- [1] Z. Szklarska-Smialowska, Corros. Sci. 41 (1999) 1743.
- [2] (a) P. Campestrini, E.P.M. van Westing, J.H.M. de Wit, Electrochim. Acta 46 (2001) 2631; (b) P. Campestrini, E.P.M. van Westing, A. Hovestad, J.H.M. de Wit, Electrochim. Acta 47 (2002) 1097.
- [3] J. Zhao, L. Xia, A. Sehgal, D. Lu, R.L. McCreery, G.S. Frankel, Surf. Coat. Technol. 140 (2001) 51.
- [4] (a) D.E. Tallman, G. Spinks, A. Dominis, G.G. Wallace, J. Solid State Electrochem. 6 (2002) 73; (b) G. Spinks, A. Dominis, G.G. Wallace, D.E. Tallman, J. Solid State Electrochem. 6 (2002) 85.
- [5] T.D. Nguyen, M. Keddah, H. Takenouti, Electrochem. Solid State Lett. 6 (2003) B25.
- [6] J. He, D.E. Tallman, G.P. Bierwagen, J. Electrochem. Soc. 151 (2004) B644.
- [7] G. Paliwoda-Porebska, M. Rohwerder, M. Stratmann, U. Rammelt, L.M. Duc, W. Plieth, J. Solid State Electrochem. 10 (2006) 730.
- [8] I.L. Lehr, S.B. Saidman, Corros. Sci. 49 (2007) 2210.
- [9] N.C.T. Martins, T. Mourae Silva, M.F. Montemor, J.C.S. Fernandes, M.G.S. Ferreira, Electrochim. Acta 53 (2008) 4754.
- [10] K.R.L. Castagno, D.S. Azambuja, V. Dalmoro, J. Appl. Electrochem. 39 (2009) 93.
- [11] (a) M. Rohwerder, A. Michalik, Electrochim. Acta 53 (2007) 1300; (b) M. Rohwerder, L.M. Duc, A. Michalik, Electrochim. Acta 54 (2009) 6075.
- [12] J.M. Gustavsson, P.C. Innis, J. He, G.G. Wallace, D.E. Tallman, Electrochim. Acta 54 (2009) 1483.
- [13] M. Rizzi, M. Trueba, S.P. Trasatti, Synth. Met. 161 (2011) 23.
- [14] S.F. Cogan, M.D. Gilbert, G.L. Holleck, J. Ehrlich, M.H. Jillson, J. Electrochem. Soc. 147 (2000) 2143.
- [15] M. Kendig, M. Hon, Corrosion 60 (2004) 1024.
- [16] M.C. Yan, D.E. Tallman, G.P. Bierwagen, Electrochim. Acta 54 (2008) 220.
- [17] M. Rohwerder, S. Isik-Uppenkamp, C.A. Amarnath, Electrochim. Acta 56 (2011) 1889.
- [18] M.A. Petrunin, A.P. Nazarov, Y.N. Mikhailovski, J. Electrochem. Soc. 143 (1996) 251.
- [19] A.M. Beccaria, L. Chiarttini, Corros. Sci. 41 (1999) 885.

- [20] W.J. van Ooij, D. Zhu, *Corrosion* 57 (5) (2001) 413.
- [21] W.J. van Ooij, D. Zhu, V. Palanivel, J.A. Lamar, M. Stacy, *Silicon Chem.* 3 (2006) 11.
- [22] E.P. Plueddemann, *Silane Coupling Agents*, 2nd ed., Plenum Press, New York, 1990.
- [23] L.M. Palomino, P.H. Suegama, I.V. Aoki, M.F. Montemor, H.G. de Melo, *Corros. Sci.* 50 (2008) 1258.
- [24] (a) M. Trueba, S.P. Trasatti, *Prog. Org. Coat.* 66 (2009) 254;  
(b) M. Trueba, S.P. Trasatti, *Prog. Org. Coat.* 66 (2009) 265;  
(c) M. Trueba, S.P. Trasatti, *J. Appl. Electrochem.* 39 (2009) 2061.
- [25] S.I. Cordoba de Torresi, A.N. Bassetto, B.C. Trasferetti, *J. Solid State Electrochem.* 2 (1998) 24.
- [26] A.J. Heeger, *J. Phys. Chem. B* 105 (2001) 8475.
- [27] (a) T. Lindfors, A. Ivaska, *J. Electroanal. Chem.* 531 (2002) 43;  
(b) T. Lindfors, A. Ivaska, *J. Electroanal. Chem.* 535 (2002) 65.
- [28] H.E. Bayer, T.L. Gall (Eds.), *Metals Handbook*, American Society of Metals, Metals Park, Ohio, 1985.
- [29] M. Trueba, S.P. Trasatti, *Mater. Chem. Phys.* 121 (2010) 523.
- [30] ASTM G31-72 (1999) Standard Practice for Laboratory Immersion Corrosion, Testing of Metals, US, 1999.
- [31] (a) J.R. Koe, M. Fujiki, *Silicon Chem.* 1 (2002) 77;  
(b) J.R. Koe, M. Motonaga, M. Fujiki, R. West, *Macromolecules* 34 (2001) 706.
- [32] J.F. Brown, P.I. Prescott, *J. Am. Chem. Soc.* 86 (1964) 1402.
- [33] T. Lin, C. He, Y. Xiao, *J. Phys. Chem. B* 107 (2003) 13788.
- [34] F.-K. Sua, J.-L. Honga, L.-L. Lin, *Synth. Met.* 142 (2004) 63.
- [35] (a) K.G. Neo, E.T. Kang, K.L. Tan, *J. Phys. Chem.* 96 (1992) 6777;  
(b) K.G. Neo, E.T. Kang, K.L. Tan, *Polymer* 34 (1993) 3921;  
(c) E.T. Kang, K.G. Neoh, K.L. Tan, *Prog. Polym. Sci.* 23 (1998) 277.
- [36] (a) A. Malinauskas, R. Holze, *Ber. Bunsenges. Phys. Chem.* 101 (1997) 1859A;  
(b) A. Malinauskas, R. Holze, *Electrochim. Acta* 43 (1998) 2413;  
(c) A. Malinauskas, R. Holze, *Electrochim. Acta* 44 (1999) 2613.
- [37] P.K. Chowdhury, *J. Phys. Chem. A* 107 (2003) 5692.
- [38] M. Trueba, S.P. Trasatti, D.O. Flamini, *Adv. Mater. Res.* 138 (2010) 63.
- [39] N. Tillman, A. Ulman, J.S. Schildkraut, T.L. Penner, *J. Am. Chem. Soc.* 110 (1988) 6136.
- [40] M.-I. Boyer, S. Quillard, E. Rebourt, G. Louarn, J.P. Buisson, A. Monkman, S. Lefrant, *J. Phys. Chem. B* 102 (1998) 7382.
- [41] K. Cory Schomburg, R.L. MacCarley, *Langmuir* 17 (2001) 1993.
- [42] R. Murugesan, E. Subramanian, *Bull. Mater. Sci.* 25 (2002) 613.
- [43] V. Jousseume, M. Morsli, A. Bonnet, *J. Appl. Polym. Sci.* 90 (2003) 3730.
- [44] B. Zhao, K.G. Neoh, E.T. Kang, *Chem. Mater.* 12 (2000) 1800.
- [45] P. Rannou, D. Rouchon, Y.F. Nicolau, M. Nechtschein, A. Ermolieff, *Synth. Met.* 101 (1999) 823.
- [46] S.N. Kumar, F. Gaillard, G. Bouyssoux, *Synth. Met.* 36 (1990) 111.